RSC Advances

PAPER

View Article Online
View Journal | View Issue

Cite this: *RSC Adv.*, 2016, **6**, 227

Comparative study of the inverse *versus* normal bicontinuous cubic phases of the β-D-glucopyranoside water-driven self-assemblies using fluorescent probes†

N. Idayu Zahid,[a] Osama K. Abou-Zied,*[b] N. A. Nabila Saari[a] and Rauzah Hashim[a]

Lipid/water systems displaying cubic symmetry are pervasive in biomembranes and important in technological applications such as nanoparticle templating and drug-delivery systems. Herein, we characterized the inverse bicontinuous cubic phase of the 2-hexyl-decyl-β-D-glucopyranoside/water system and the normal bicontinuous cubic phase of the octyl-β-D-glucopyranoside/water system. We investigated the head group region using 2-(2′-hydroxyphenyl)benzoxazole (HBO) and two of its derivatives as fluorescent probes. In the inverse phase, the *syn*-enol tautomer of HBO dominates the signal. This is attributed to the very narrow water channels (diameter of 2.3 nm) which support the formation of a hydrogen bond between the OH group of HBO and oxygen from the sugar units. A small contribution from the HBO anion species was also detected and is proposed to be the result of a hydrogen ion abstraction by the sugar units. In contrast, fluorescence of HBO in the normal phase is dominated by the keto tautomer with some contribution from the anionic form. Fluorescence lifetimes indicate that efficient excited-state intermolecular proton transfer, facilitated by the confined water molecules, yields the keto tautomer. This confined water contributes also toward the stability of the anion species in both cubic phases. Attaching a C_4 (HBO-C_4) or a C_8 (HBO-C_8) alkyl chain to the phenyl ring of HBO yielded similar results which indicates that the HBO moiety occupies the same position in the hydrophilic region, regardless of the attached hydrophobic chain. The two detected forms of HBO in each lipid suggest a degree of local heterogeneity that was also observed in the measured two fluorescence lifetime components. The current study is anticipated to contribute toward a better understanding of drug–lipid interaction which is important for drug absorption by the cell membrane.

Received 24th September 2015
Accepted 1st December 2015

DOI: 10.1039/c5ra19794e

www.rsc.org/advances

Introduction

Dispersion of lipids in water assumes a variety of lamellar and non-lamellar liquid crystalline structures (*e.g.* cubic, hexagonal, and ribbon phases).[1–3] The addition of additives or other components into these binary systems may lead to the formation of stable colloidal dispersions such as vesicles, cubosome and hexosome emulsions.[4–7] One of the most structurally interesting lyotropic mesophases adopted by lipids is the bicontinuous cubic symmetry which can be either normal (Type I) or inverse (Type II). In the normal structure, the interface curves towards the hydrophobic chain region while the inverse gives a curvature towards the polar aqueous region. A bicontinuous cubic phase consists of a continuous bilayer which divides the aqueous component into two interpenetrating but unconnected water channels of nanometric size. Also called a triply periodic minimal surface (TPMS), it is sub-divided into the "diamond" (D), the "primitive" (P) and the "gyroid" (G), with space groups of *Pn3m*, *Im3m* and *Ia3d*, respectively. These phases are important in many biologically processes such as fusion and fat digestion.[8–11] For example, intercellular lipid membranes adopt the gyroid structure.[12–14]

The inverse structures accommodate both hydrophobic or hydrophilic biomolecules such as drugs, proteins, peptides and nucleic acids.[15–19] Their amphiphilicity, high interfacial area, specific and controllable water channel sizes leads to a remarkable efficiency for loading of guest molecules and easy passage for bioactive species.[8,20,21] These unique features can be exploited for many technological applications,[22–25] including encapsulation of drugs in nanometric structures.[18,26,27] Furthermore, in delivering a liposoluble drug, the lipid may ionize or protonate small molecules that will influence the drug's neutral state and its ability to cross the lipidic membrane. For example, the pH in the vicinity of the

[a]*Department of Chemistry, Faculty of Science, University of Malaya, 50603 Kuala Lumpur, Malaysia*

[b]*Department of Chemistry, Faculty of Science, Sultan Qaboos University, P.O. Box 36, 123, Muscat, Sultanate of Oman. E-mail: abouzied@squ.edu.om*

† Electronic supplementary information (ESI) available. See DOI: 10.1039/c5ra19794e

membrane environment may reflect the local heterogeneity which influences the ionization state of neighbouring molecules such as drugs.[28–30] Unionized drugs are lipid soluble and diffusible, able to cross the membrane's lipid bilayer, unlike the charged species.[31–33] Therefore, it is important to know the degree of ionization of a drug molecule as a consequence of changes within its environment due to pH or polarity. Hence a systematic study of the lipid–drug interaction is necessary.[34–36] The current study is a step in this direction.

We have recently studied a model of an inverse gyroid cubic phase with a *Ia3d* space group formed by the branched chain Guerbet glycoside (2-hexyl-decyl-β-D-glucopyranoside (β-Glc-$OC_{10}C_6$)) by using fluorescent probes, tryptophan and its derivatives.[37] From the steady-state and time-resolved fluorescence methods, the tryptophan fluorescence signals show an unusual local basic environment inside the nano-channels that is equivalent to a solution of pH ≥ 10.0. The basic effect is attributed to the restricted motion of water in the narrow nano-channels. These restricted water molecules are located very close to the OH groups of the sugar units. Such a confinement promotes the transfer of highly polar substances, such as ions, to the cells.[37]

In order to further clarify the previously observed unusual basic effect, we investigate in this work the ability of the Type II inverse bicontinuous cubic phase of β-Glc-$OC_{10}C_6$ (*Ia3d* space group) to stabilize different chemical structures of an encapsulated ligand and its ability to affect the ligand's neutral state in the polar nano-channels using steady-state and time-resolved fluorescence methods. The β-Glc-$OC_{10}C_6$ lipid (shown in Fig. 1) consists of a single sugar unit with a branched alkyl chain of 16 carbon atoms, which closely bear a structural resemblance to the natural products such as monogalactosyldiacylglycerol (MGDG) and digalactosyldiacylglycerol (DGDG) from the photosynthetic thylakoid membrane.[38] In order to understand the effect of the structural packing on the ligand's fluorescence, we carry out the same experiments on the Type I normal cubic phase of the octyl-β-D-glucopyranoside (β-Glc-OC_8) lipid (Fig. 1) which will help in understanding the similarities and differences between the two cubic self-assemblies. For this purpose, we employed 2-(2′-hydroxyphenyl)benzoxazole (HBO, shown in Fig. 2(a)) as a fluorescent probe. The complex photophysics and the distinguished fluorescence signatures of the different tautomeric forms of HBO make this molecule a potential probe to report on its immediate environment. To test the accessibility of HBO in different regions within the lipid head group in the hydrophilic domain, we attached a C_4 (HBO-C_4) and a C_8 (HBO-C_8) alkyl chain to the phenyl ring of the HBO parent molecule. Fig. 2(b) shows the structures of the new HBO derivatives.

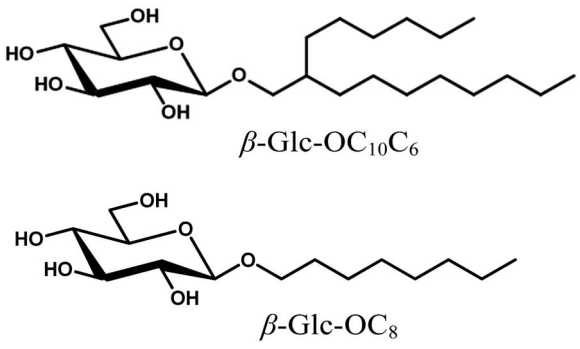

Fig. 1 Lipids' chemical structures of 2-hexyl-decyl-β-D-glucopyranoside (β-Glc-$OC_{10}C_6$), which gives Type II and octyl-β-D-glucopyranoside (β-Glc-OC_8), which gives Type I.

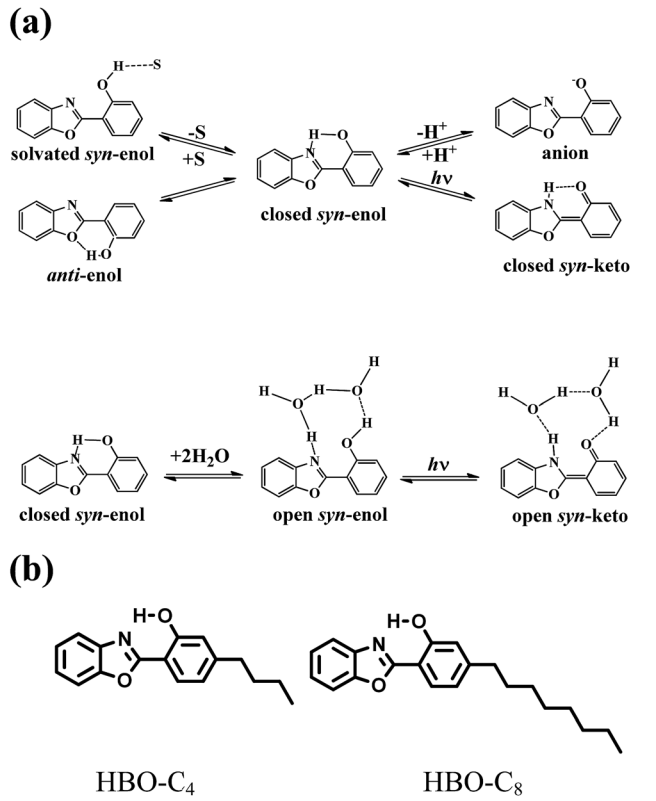

Fig. 2 (a) Tautomeric forms of HBO, where S represents polar solvents. (b) Chemical structures of the new probes of HBO derivatives.

HBO is one of the benzazole molecules[39,40] which are known to have inhibition effect on several enzymatic reactions and are reported to treat some diseases.[41,42] This unique inhibitory activity is attributed to the presence of the N-heteroatom in the structural backbone that can act as both proton donor and/or acceptor.[43] Fig. 2(a) shows the different tautomeric forms of the HBO molecule.[44–51] In the ground state, the molecule exists in a conformational equilibrium between the *syn*- and *anti*-enols. The phenyl group of the *syn*-enol tautomer may form a closed *syn*-enol tautomer (intramolecular hydrogen bond) or a solvated *syn*-enol species (intermolecular hydrogen bond with solvent). Only the closed *syn*-enol efficiently forms the closed *syn*-keto tautomer upon photoinduced excitation (excited-state intramolecular proton transfer (ESIPT)). In hydrophobic solvents which are unable to solvate the phenolic proton, excitation results in an efficient ESIPT with a Stokes' shifted fluorescence.

However, in protic solvents, which are able to solvate the phenolic proton, emission from both the enol and the keto tautomers are observed with intensities that depend on the concentration of the closed *syn*-enol relative to the solvated *syn* and *anti*-enol tautomers. On the other hand, the formation of the open *syn*-enol tautomer is more favourable in aqueous medium. Two water molecules solvate the hydrogen bonding sites of this tautomer and transforms the molecule into the open *syn*-keto tautomer upon excitation (see Fig. 2(a)).[51] The anion form of HBO was detected in basic medium and in binary solvents with a unique fluorescent peak that lies between those of the enol and the keto tautomers.[51]

For clarity, we included the published phase diagrams of both β-Glc-$OC_{10}C_6$ [52] and β-Glc-OC_8 [53] in the ESI (Fig. S1†). The lattice parameter of the inverse cubic phase (Type II) of β-Glc-$OC_{10}C_6$ at 20% (w/w) was found to be 7.6 nm,[52] while that for the normal cubic phase (Type I) of β-Glc-OC_8 is of about 7.3 nm at 21% (w/w).[53] In the present study, both phases have similar water content, but in Type II the bicontinuous network region are filled with water while the lipid chains occupy the matrix region. Conversely, in Type I, the network region is hydrophobic, filled with the lipid tails, while the intermediate space is filled with the hydrophilic sugar heads and water.[54,55]

Experimental section

Materials

The synthesis of β-Glc-$OC_{10}C_6$ is described elsewhere[56] and the anomeric purity of the lipid was confirmed to be ≥98% according to ^{1}H NMR, ^{13}C NMR and thin layer chromatography. NMR data for the lipid are available in the ESI.† β-Glc-OC_8 (98%), HBO (98%) and D-glucose (96%), anhydrous dioxane, DMSO, methanol and cyclohexane were all obtained from Sigma-Aldrich. HBO-C_4 and HBO-C_8 were custom-made by GlycoTeam GmbH, Germany.[57] The purity of both derivatives was estimated to be ≥98%. All chemicals and solvents were used without further purification.

Sample preparation

The concentration of HBO and its derivatives in the β-Glc-$OC_{10}C_6$/water and β-Glc-OC_8/water systems for both steady-state and time-resolved experiments was adjusted to 0.1 mM. The value was based on an estimated density of ~1.0 g mL^{-1} for the mixture. According to their previously published phase diagrams, both inverse and normal bicontinuous cubic phases used for this study were observed at 20% (w/w) water content of β-Glc-$OC_{10}C_6$/water[52] and β-Glc-OC_8/water[53,58,59] systems, respectively (see Fig. S1 in the ESI†). The cubic phases were confirmed to be formed by illuminating the sample in the flame-sealed tube and examining it through a cross-polarizing filter. The cubic phase samples were optically isotropic under the cross-polarizing filter and highly viscous. These two properties are characteristic of the cubic lipid phases. All samples were treated with the same procedure used in our previous work.[37,57,60,61] The aqueous buffer used was 25 mM sodium phosphate buffer, pH 7.2. The samples included the lipid mixed with the different probes, in addition to one sample with no probe which was used as a standard in the measurements. For HBO and D-glucose samples in solution, a stock solution in methanol (10 mM) for the former and in buffer (10 mM) for the latter were prepared. These solutions were then diluted with buffer to reach the desired concentrations. The final methanol : H_2O (v/v) mixture was 10 : 90. A ratio above 20 : 80 was shown to have similar properties of pure water.[51,62]

Instrumentation

Fluorescence spectra were recorded on a Shimadzu RF-5301 PC spectrofluorophotometer. Lifetime measurements were performed using a TimeMaster fluorescence lifetime spectrometer obtained from Photon Technology International. Excitation was performed at 340 nm and 380 nm using light-emitting diodes. The instrument response function (IRF) was measured from the scattered light and estimated to be approximately 1.5 ns (full-width at half-maximum). The measured transients were fitted to a multiexponential function (eqn (1)), convoluted with the system response function ($L(t)$).

$$I(t) = \sum_i \alpha_i \ \exp(-t/\tau_i) \quad (1)$$

In this expression, the values of α_i are the relative amplitudes (pre-exponential factors) and the τ_i values are the fluorescence lifetimes. $\sum_i \alpha_i$ is normalized to unity and represents the relative contribution of the lifetime values to the overall decay transient. The fit was judged by the value of the reduced chi-squared (χ^2). The experimental time resolution (after deconvolution) was approximately 100 ps, using stroboscopic detection, where the observed decay ($I(t)_{obs}$) is expressed as:[63]

$$I(t)_{obs} = \int_0^t L(t-s)I(s)\mathrm{d}s \quad (2)$$

In the current work, two lifetime components produced the best fits in all cases (Fig. 4 and 7, and Table 1, *vide infra*). In all the experiments, samples were measured in a 1 cm path-length quartz cell at 23 ± 1 °C.

Results and discussion

Spectroscopy of the HBO probes in neutral and basic aqueous solutions

The steady-state and time-resolved spectroscopy of HBO was thoroughly investigated in different solvents,[44–51] DNA,[64,65] protein,[66,67] and in lipids.[57] We included the absorption and fluorescence spectra of HBO in different solvents in the ESI (Fig. S2 and S3,† respectively). For the current work, it is important to understand the fluorescence behaviour of HBO, HBO-C_4 and HBO-C_8 in aqueous medium before the study is carried out in lipids due to the high water composition in all the lipidic systems studied here. From our previous study on HBO,[51,66,67] fluorescence in neutral and basic aqueous media is simple with only one species dominating in each case. We

Table 1 Fluorescence lifetime measurements of HBO and its derivatives in solution, inverse cubic phase (β-Glc-$OC_{10}C_6$) and normal cubic phase (β-Glc-OC_8)

		Lifetime, τ		
Probe	λ (detection)	τ_1[a] keto	τ_2[b] anion	τ_3[c] solvated *syn*-enol
HBO in buffer pH 7.2		5.5[d]		
HBO in buffer pH 12.0			2.6[d]	
HBO-C_4 in buffer pH 7.2		5.5		
HBO-C_4 in buffer pH 12.0		5.1 (0.55)	1.3 (0.45)	
HBO-C_8 in buffer pH 7.2		6.1[d]		
HBO-C_8 in buffer pH 12.0		6.1 (0.74)[d]	1.3 (0.26)[d]	
Inverse cubic				
HBO	≥380 nm		0.8 (0.19)	8.4 (0.81)
	≥515 nm		0.8 (0.49)	8.4 (0.51)
HBO-C_4	≥380 nm		0.8 (0.28)	7.6 (0.72)
	≥515 nm		0.8 (0.60)	7.6 (0.40)
HBO-C_8	≥380 nm		0.8 (0.25)	7.7 (0.75)
	≥515 nm		0.8 (0.56)	7.7 (0.44)
Normal cubic				
HBO	≥380 nm	3.9 (0.50)	0.6 (0.50)	
	≥515 nm	3.9 (0.50)	0.6 (0.50)	
HBO-C_4	≥380 nm	3.6 (0.47)	0.7 (0.53)	
	≥515 nm	3.6 (0.49)	0.7 (0.51)	
HBO-C_8	≥380 nm	3.6 (0.49)	0.8 (0.51)	
	≥515 nm	3.6 (0.51)	0.8 (0.49)	

[a] ± 0.2 ns; [b] ± 0.1 ns; [c] ± 0.2 ns. Relative contributions are listed in parentheses. [d] Values were taken from ref. 57. λ_{ex} = 340 nm. In solution, fluorescence was detected using 380 nm long-path filter while in lipid, fluorescence was detected using either 380 nm or 515 nm long-path filters as mentioned in the table.

carried out a fluorescence study on aqueous solutions of HBO-C_4 and HBO-C_8 in order to investigate the effect of the alkyl chain length attached on the parent HBO molecule. Fig. 3 displays the results in pH 7.2 and 12.0. In neutral pH, the fluorescence behaviour of HBO derivatives in general is similar to that of HBO, except for a slight blue shift of the keto fluorescence peak in the former. On the other hand, in basic aqueous medium the fluorescence behaviour is different for HBO derivatives. Unlike HBO where there is a complete anion formation in pH 12.0 (peak at ~440 nm), the fluorescence behaviour of HBO-C_4 and HBO-C_8 shows that the keto tautomer dominates the fluorescence signal in pH 12.0 (peak at ~470 nm) with a small contribution from the anion species. As shown in Fig. 3, HBO-C_4 shows a higher intensity for the anion fluorescence compared to HBO-C_8. The results are in substantial agreement with our recently reported data on HBO and two of its derivatives (including HBO-C_8).[57] The less contribution from the anion species in HBO-C_8 to the overall fluorescence signal, compared to that in HBO-C_4, points to the effect of the chain length attached to the phenyl ring in destabilizing the ionized form of HBO. This may be due to an enhanced inductive effect as the chain length gets longer, providing more negative charge to the delocalized π-electrons.

The fluorescence decay transients for HBO and its derivatives are shown in Fig. 4 for aqueous solutions of pH 7.2 and 12.0. The lifetime data are summarized in Table 1. In neutral pH, HBO and its derivatives show lifetime values (τ_1) that are

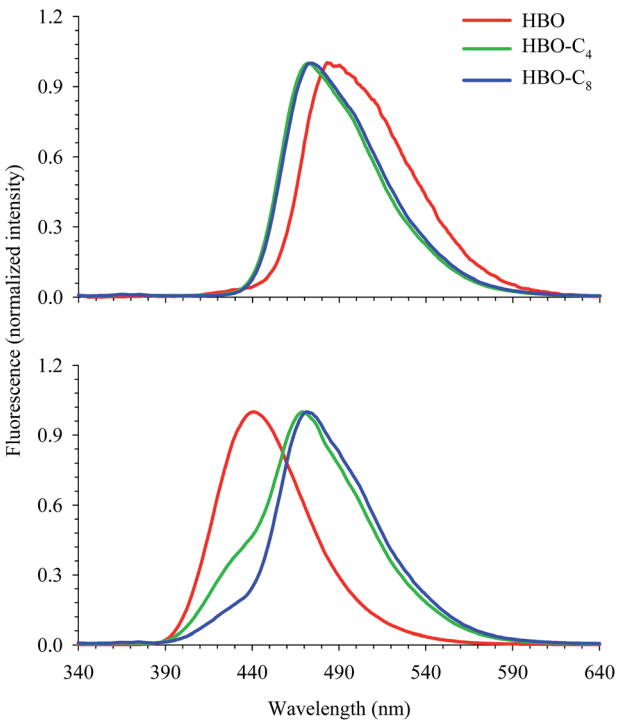

Fig. 3 Fluorescence spectra of HBO and its derivatives in aqueous solutions of pH 7.2 (upper segment) and pH 12.0 (lower segment). λ_{ex} = 330 nm.

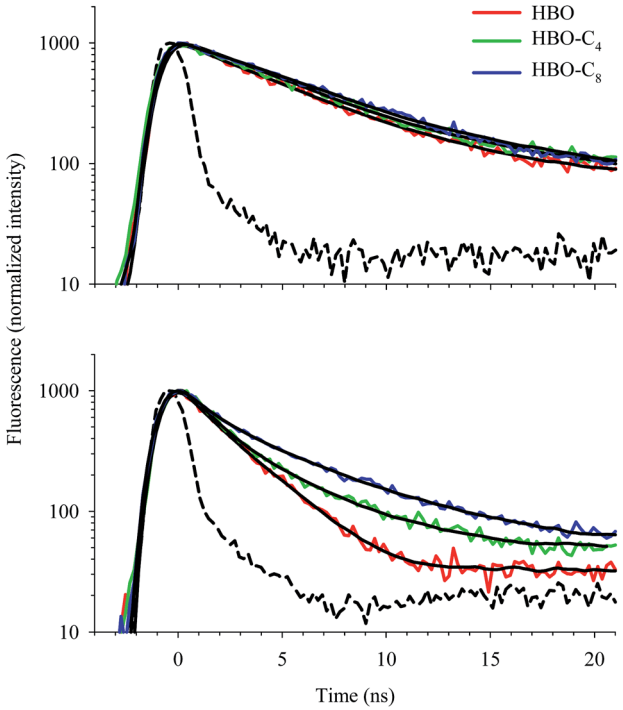

Fig. 4 Decay transients of HBO and its derivatives in aqueous solutions of pH 7.2 (upper segment) and pH 12.0 (lower segment). λ_{ex} = 340 nm. Signal was measured using a 380 nm long-path filter. IRF is shown in a dashed line. Black solid lines represent the best fits.

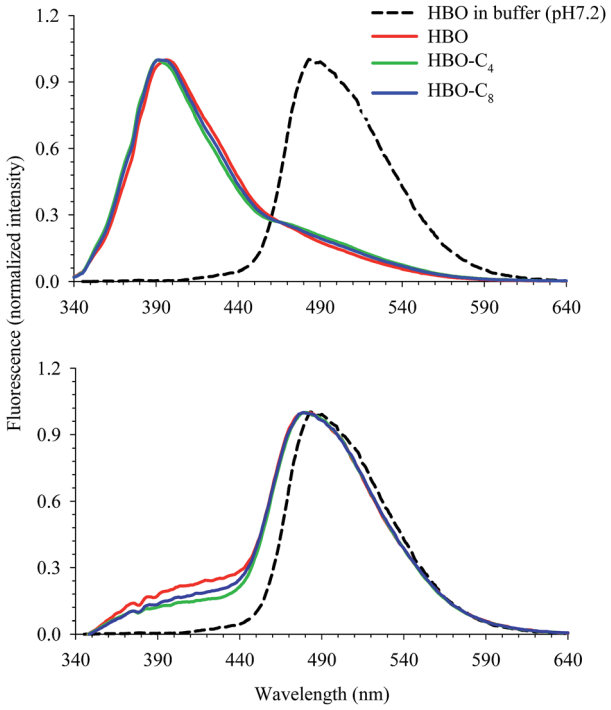

Fig. 5 Fluorescence spectra of HBO and its derivatives in inverse cubic phase "β-Glc-$OC_{10}C_6$" (upper segment) and normal cubic phase "β-Glc-OC_8" (lower segment). The spectrum of HBO in aqueous solution of pH 7.2 is included for comparison. λ_{ex} = 330 nm.

consistent with the formation of the open *syn*-keto (water-assisted tautomerization), as previously assigned.[66,67] In aqueous solution of pH 12.0, one lifetime component in the fluorescence decay transient of HBO was assigned to the anionic form (2.6 ns).[51,57] For HBO-C_4 and HBO-C_8, fitting the transient decay curves gives a major contribution from the open *syn*-keto tautomer (5.5 ns for HBO-C_4 and 6.1 ns for HBO-C_8) and a small contribution from the anion form (1.3 ns) as shown in Table 1. The current assignments are consistent with our recent assignments for HBO-1 (C_8 attached to the benzoxazole ring) and HBO-2 (C_8 attached to the phenyl ring).[57] The larger contribution from the anion species in HBO-C_4 (45%) compared to that in HBO-C_8 (26%) is in agreement with the observed relative intensities of the different species in the steady-state results (Fig. 3).

The above results will be used in the remaining sections as references for understanding the local environment in lipids when HBO and its derivatives are used as probes.

Steady-state fluorescence probing of the head group regions

The fluorescence spectra of HBO, HBO-C_4 and HBO-C_8 incorporated inside the inverse cubic phase of β-Glc-$OC_{10}C_6$ and normal cubic phase of β-Glc-OC_8 with the *Ia3d* space group are shown in Fig. 5 for λ_{ex} = 330 nm. The spectra of HBO in neutral and basic aqueous solutions are included for comparison. A striking difference in the behaviour of HBO is clear in the major contribution from the enol fluorescence in the Type II inverse cubic phase to the overall signal, whereas the keto signal dominates the fluorescence spectrum in the Type I normal cubic phase. In both cases, a shoulder at the red side (inverse phase) or the blue side (normal phase) can clearly be observed. The shoulder can be assigned to one or more of the other tautomers of HBO. It is clear that the shoulder in each lipid has a similar spectral location as that of the HBO anion. In order to clarify the assignment of the shoulder peaks, we display in Fig. 6 (upper segment) the fluorescence spectra of HBO in the two lipids, as well as in aqueous solutions of glucose and in different pHs. The HBO molecule shows a slight contribution from the anion species in the presence of glucose. This observation indicates that an intermolecular proton transfer from HBO to glucose is a possible mechanism for the formation of the HBO anion. We have shown recently that maltose induces a similar effect on HBO in solution.[57] We have also reported recently a similar basic effect for the inverse cubic phase using tryptophan as a fluorescent probe.[37] This effect was attributed to the restricted motion of water in the nano-channels (diameter of 2.3 nm) in which water molecules are situated very close to the OH groups of the sugar units. The formation of the anion species of HBO in neutral sugar solution must then be a consequence of the amphoteric character of sugar in aqueous environment. In addition, the constrained water in this region has a solvation effect that is quite different from that of free, bulk water. In β-cyclodextrin, which is composed of seven glucose units, it has been reported that water near the cavity rim is affected by the extensive network of the OH groups of the sugar units and tends to be basic.[68] The basic effect of the

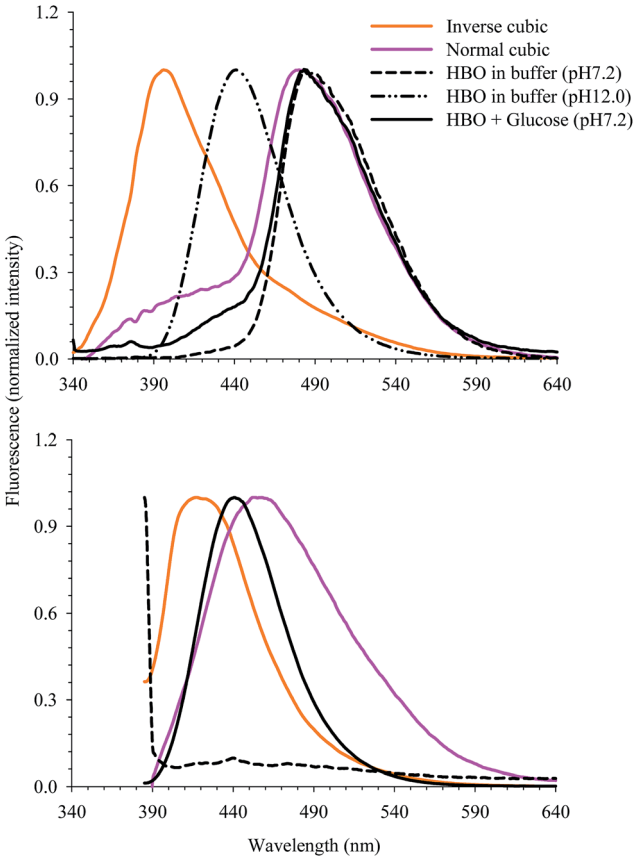

Fig. 6 Upper segment: fluorescence spectra of HBO in buffer solutions of pH 7.2 and pH 12.0, inverse cubic phase (β-Glc-$OC_{10}C_6$), normal cubic phase (β-Glc-OC_8), and mixed with glucose (1 : 1 molar ratio) in neutral buffer. λ_{ex} = 330 nm. Lower segment: HBO in buffer solutions of pH 7.2 and pH 12.0, inverse cubic phase (β-Glc-$OC_{10}C_6$), and normal cubic phase (β-Glc-OC_8). λ_{ex} = 380 nm.

confined water may also lead to the formation of the anion species of HBO in the cubic phases. As shown in Fig. 5, the presence of the alkyl chains (C_4 and C_8) have no apparent effect on the fluorescence signal in each lipid which implies similar location of the HBO moiety in each self-assembly. This observation is quite different from our reported study on maltoside self-assemblies in which the presence of two sugar units (disaccharide) increases the area of the polar head group, allowing the probe molecule to be situated in different regions.[57]

In order to confirm the above assignments, we measured the fluorescence spectra after excitation at 380 nm, where the absorption peak of only the anion species of HBO is located.[51,66] The spectra are shown in Fig. 6 (lower segment) for HBO in different environments. It is clear that HBO has no fluorescence in neutral buffer, whereas fluorescence is detected in both lipids. The fluorescence spectra in lipids also show similar structural peaks to those measured after excitation at 330 nm (Fig. 5), with more contribution from the anion species at ~440 nm. The results confirm the formation of the anion species in both lipid self-assemblies in neutral pH. The stability of the anion form can be a consequence of the strong interaction between the OH group of HBO and the polar sugar head groups. As reported in our recent work[57] and mentioned above, the head group region of different lipidic forms induces an ionization ability on the adjacent probes. This ability was attributed to the packing effect of the sugar units, in addition to the confined water molecules. The current results imply that the equilibrium between two species of HBO in each lipid in the excited state is supported by the close proximity between the polar sites of HBO and those of the sugar units. In such case and in neutral pH, excitation of the anion species at 380 nm will still lead to the formation of the neutral tautomer in the excited state by intermolecular proton transfer.

Time-resolved fluorescence study

Fluorescence lifetime measurements of HBO and its derivatives are summarized in Table 1. The transients for HBO in the inverse and normal cubic phases, as well as in neutral buffer, are displayed in Fig. 7. The complex photophysics of HBO makes it a useful probe to report on its immediate vicinity, on the other hand care must be taken when assigning the lifetime data to their respective tautomeric forms. Accordingly, our lifetime assignments in lipids are based on the thoroughly studied dynamics of HBO in different environments.[44–51,64–67]

The decay profile of HBO and its derivatives in the inverse cubic phase is biexponential and the two lifetime components are due to the *syn*-enol (7.6–8.4 ns) and the anion species (0.8 ns). We confirmed the assignments by measuring the decay profiles after using a long-path filter of 515 nm. As shown in Table 1, the contribution from the anion species is much larger because the observation window is located more in the spectral region of the anion species. The fluorescence lifetime values in Table 1 (τ_3) indicate that the enol band is due solely to the solvated *syn*-enol as the lifetime of the *anti*-enol tautomer (fluoresces in the same spectral region) is reported to be 1.5 ns and solvent-independent.[45] Since this band is absent in buffer

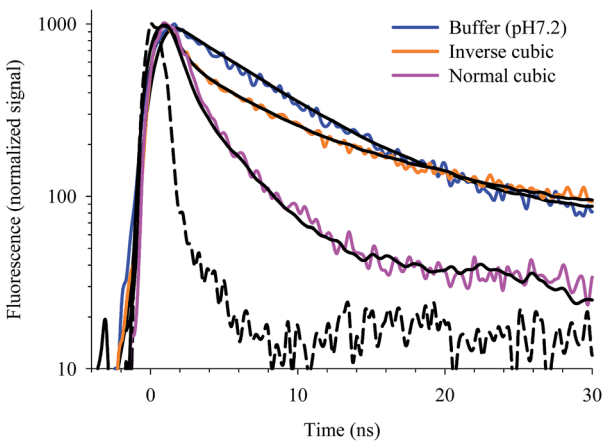

Fig. 7 Fluorescence decay transients of HBO in inverse cubic phase (β-Glc-$OC_{10}C_6$) and normal cubic phase (β-Glc-OC_8). The decay transient of HBO in buffer pH 7.2 is included for comparison. λ_{ex} = 340 nm. Signal was measured using a 380 nm long-path filter. IRF is shown in a dashed line. Black solid lines represent the best fits.

alone for all the HBO probes (Fig. 3), it must derive from intermolecular hydrogen bond interaction between the OH group of HBO and the polar sites of the sugar units in lipids. The relatively much longer lifetime values for this tautomer (about 26 times) compared to the reported values for HBO in different solvents[44,45,48–50] is a manifestation of the different mechanism of interaction, where oxygen from the sugar head groups is involved.

In contrast to the inverse cubic phase, the steady-state fluorescence spectra of the HBO probes in the normal cubic phase show a major contribution from a Stokes-shifted peak at 480 nm (Fig. 5) which is due to the keto tautomer that is formed after ESIPT. Two lifetime components were measured for HBO in the normal cubic phase as shown in Table 1. The short component is assigned to the anion lifetime (0.6–0.8 ns), similar to that observed in the inverse phase, while the long component is assigned to the keto tautomer (3.6–3.9 ns). The contribution from each species is about 50%, and using different long-path filters did not distinguish between the two forms. This observation can be attributed to the large overlap between the spectral regions of the two species.

The stability of different tautomeric forms of HBO in each cubic phase self-assembly is indicative of the different local environment in the head group region. Similar results were reported when HBO was used as a local reporter in the minor groove of a DNA duplex in which preferential stabilization of the solvated *syn*-enol tautomer was observed.[65] This was attributed to the formation of a hydrogen bond between the OH group of HBO and the O4′ atom of an adjacent nucleotide. On the other hand, when HBO was placed in the major groove of the same DNA double helix, the keto tautomer dominated the fluorescence signal.[64] In the present work, the stability of the *syn*-enol form of HBO in the inverse cubic phase (Type II) indicates a close interaction between the OH group of HBO and an oxygen atom in an adjacent sugar unit as mentioned above. This intermolecular hydrogen bond will hinder the formation of the keto tautomer since the intramolecular hydrogen bond in HBO is disrupted. The same mechanism of interaction may also lead to the anion formation since the oxygen atom of the OH group becomes more acidic in the excited state.[69] The proton transfer occurs as soon as the H atom comes within the chemical interaction range of the other electronegative atom in sugar. We have observed previously the formation of solvated *syn*-enol and the anion tautomers through a similar mechanism in lipidic phases of dodecyl-β-D-maltoside.[57]

On the other hand, the population of the keto tautomer in the Type I normal cubic phase can be the result of either ESIPT (closed *syn*-enol → closed *syn*-keto; Fig. 2(a)), or by an assisted tautomerization *via* water molecules (open *syn*-enol → open *syn*-keto; Fig. 2(a)). The former mechanism implies a large degree of isolation of the HBO molecule in a hydrophobic environment. This case was reported for HBO in the major groove of a DNA duplex as mentioned earlier, where the keto lifetime was measured to be 5.0 ns (at least 17 fold longer than the keto lifetimes in solvents).[64] However, this may not be the case in the present study, since HBO appears to interact with the polar sites of the sugar head groups (anion formation). The possible mechanism is then the formation of the keto tautomer in the normal cubic phase by intermolecular proton transfer that involves water. The major contribution from this keto tautomer to the overall fluorescence signal must be a consequence of the close proximity of the HBO polar sites to water. The difference in the lifetime values of the keto tautomers in lipid (3.6–3.9 ns) from those in buffer (5.5–6.1 ns) indicates the unique local environment in lipids where water molecules are less flexible, compared to bulk water. The constrained water has a solvation effect that is quite different from that of free, bulk water.[70]

We measured the lifetime transients of HBO in lipids after excitation of the anion species in the ground state at 380 nm. The decay transients are shown in Fig. S4 in the ESI.† The biexponential nature of all the transients, with similar lifetimes and contributions as those measured above after excitation at 330 nm, reflects the kinetics accessibility of the different tautomers in the excited state, regardless of the excitation energy. The data are summarized in Table S1 in the ESI.†

Comparison between glucoside and maltoside normal cubic phases

Comparing the fluorescence spectrum of HBO in the normal cubic phase of β-Glc-OC_8 with that in dodecyl-β-D-maltoside lipid (β-Mal-OC_{12}) from our previous work[57] shows some similarities and differences. The spectra are displayed in Fig. 8. In both lipids, HBO shows a dominant fluorescence peak of the keto tautomer at 480 nm and a small concentration from the anionic form (400–440 nm). However, in the normal cubic phase of β-Mal-OC_{12}, the solvated *syn*-enol tautomer was detected in the 370–380 nm region. The additional tautomer in the maltoside lipid can be explained as the result of the disaccharide nature of the head group which has more polar sites to interact with the OH group of HBO to form the solvated *syn*-enol tautomer. This mechanism was not possible in the glucoside lipid due to the shorter head group (monosaccharide). The more pronounced anion contribution in the glucoside lipid (49–53%) than that in the maltoside lipid (10–18%)[57] may indicate

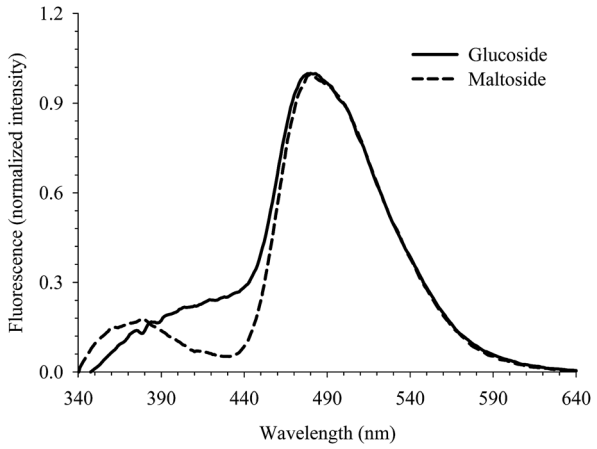

Fig. 8 Fluorescence spectra of HBO in normal cubic phases of glucoside and maltoside. λ_{ex} = 330 nm.

that any formed enol in the former undergoes a spontaneous ionization to yield the anion species. This can be a result of the more rigid monosaccharide units in glucoside, whereas the presence of the disaccharide units in maltoside inherits more flexibility to the lipidic structure. We indicated recently that the larger head group in a maltoside vesicle increases the membrane fluidity, leading to a more flexible vesicle with more leakage efficiency.[7] The larger disaccharide unit may also lead to different polarity regions. In our previous study using tryptophan (Trp) and two of its derivatives as probes, we showed that the glucose unit is too short to show any polarity gradient. On the other hand, the maltose unit is large enough to cause the tryptophan molecule in Trp-C_8 to probe deep in the head group region where the polarity approaches that of tryptophan solvated in dioxane.[60,61]

We should mention here that resolving multiexponential decay transients to their respective lifetime components is sometimes very challenging when more than one component are close in value. This was the case for HBO and two of its derivatives in dodecyl-β-D-maltoside lipid.[57] Also, comparison of lifetimes of the same species of the probe in different lipidic forms becomes difficult due to the different local environments. In the current work, the keto tautomer of HBO in the inverse cubic phase may contribute to the overall fluorescence signals and decay transients which was not possible to resolve. Similarly, the enol tautomer may have some contribution in the HBO fluorescence in the normal cubic phase. Nevertheless, the observation of more than one tautomeric form of HBO in both lipids points to the local heterogeneity in the polar region which is the result of the lipid self-assembly.[71,72] Sugar amphoterism is likely to be responsible for the induced-heterogeneity which is an important mechanism in performing the different biological functions of the membrane such as the delivery of nutrients and drugs of different molecular structures, sizes, and polarities.[73]

Conclusions

In this work, we characterized the polar nano-channels of the inverse bicontinuous cubic phase of the β-Glc-$OC_{10}C_6$ lipid using HBO and two of its derivatives (HBO-C_4 and HBO-C_8) as fluorescent probes. The microscopic nature of the head group region of the inverse cubic phase is compared to that of the normal cubic phase of β-Glc-OC_8 lipid. The results in the former show the stability of the solvated *syn*-enol and the anionic form of HBO while in the latter, the keto tautomer and the anion species are detected. The multi-tautomeric configurations of the HBO molecule in both lipid self-assemblies reflect the local heterogeneity nature of the head group regions which can be correlated to the inherited nature of the sugar amphoterism. The detected HBO anions in both cubic phases and in other lipidic structures points to the presence of a common ionization ability due to the packing structures of the lipidic self-assemblies. The induced local heterogeneity and ionization ability in lipids may affect the delivery state of molecules such as drugs. The current study is then anticipated to contribute toward a better understanding of drug–lipid interaction and drug absorption by the cell membrane.

Acknowledgements

We thank The Research Council of Oman (RC/SCI/CHEM/14/01), High Impact Research Grant (UM.C/HIR/MOHE/SC/11), and University of Malaya Research Grant (RG329-15AFR) for supporting this work.

Notes and references

1 J. M. Seddon, *Biochim. Biophys. Acta*, 1990, **1031**, 1–69.
2 H. Chung and M. Caffrey, *Nature*, 1994, **368**, 224–226.
3 G. C. Shearman, N. J. Brooks, G. J. T. Tiddy, M. Sztucki, R. H. Templer, R. V. Law, O. Ces and J. M. Seddon, *Soft Matter*, 2011, **7**, 4386–4390.
4 N. Ahmad, R. Ramsch, J. Esquena, C. Solans, H. A. Tajuddin and R. Hashim, *Langmuir*, 2012, **28**, 2395–2403.
5 X. Gong, M. J. Moghaddam, S. M. Sagnella, C. E. Conn, X. Mulet, S. J. Danon, L. J. Waddington and C. J. Drummond, *Soft Matter*, 2011, **7**, 5764–5776.
6 N. F. K. Aripin, J. W. Park and H. J. Park, *Colloids Surf., B*, 2012, **95**, 144–153.
7 M. Salim, O. K. Abou-Zied, H. U. Kulathunga, A. Baskaran, U. R. Kuppusamy and R. Hashim, *RSC Adv.*, 2015, **5**, 55536–55543.
8 V. Luzzati, *Curr. Opin. Struct. Biol.*, 1997, **7**, 661–668.
9 S. Hyde, Z. Blum, T. Landh, S. Lidin, B. W. Ninham, S. Andersson and K. Larsson, *The Language of Shape: The Role of Curvature in Condensed Matter: Physics, Chemistry and Biology*, Elsevier Science B.V., Amsterdam, 1997.
10 T. Landh, *FEBS Lett.*, 1995, **369**, 13–17.
11 J. Kraineva, V. Smirnovas and R. Winter, *Langmuir*, 2007, **23**, 7118–7126.
12 P. J. F. Gandy and J. Klinowski, *Chem. Phys. Lett.*, 2000, **321**, 363–371.
13 J. M. Thomas, O. Terasaki, P. L. Gai, W. Zhou and J. Gonzalez-Calbet, *Acc. Chem. Res.*, 2001, **34**, 583–594.
14 M. Salim, N. I. Zahid, C. Y. Liew and R. Hashim, *Liq. Cryst.*, 2015, DOI: 10.1080/02678292.2015.1085104.
15 A. Angelova, B. Angelov, S. Lesieur, R. Mutafchieva, M. Ollivon, C. Bourgaux, R. Willumeit and P. Couvreur, *J. Drug Delivery Sci. Technol.*, 2008, **18**, 41–45.
16 J. Clogston, G. Craciun, D. J. Hart and M. Caffrey, *J. Controlled Release*, 2005, **102**, 441–461.
17 L. B. Lopes, D. A. Ferreira, D. de Paula, M. T. J. Garcia, J. A. Thomazini, M. C. Fantini and M. V. L. Bentley, *Pharm. Res.*, 2006, **23**, 1332–1342.
18 J. C. Shah, Y. Sadhale and D. M. Chilukuri, *Adv. Drug Delivery Rev.*, 2001, **47**, 229–250.
19 D. McLoughlin, M. Impéror-Clerc and D. Langevin, *ChemPhysChem*, 2004, **5**, 1619–1623.
20 A. I. Tyler, H. M. Barriga, E. S. Parsons, N. L. McCarthy, O. Ces, R. V. Law, J. M. Seddon and N. J. Brooks, *Soft Matter*, 2015, **11**, 3279–3286.
21 J. L. Nieva, A. Alonso, G. Basáñez, F. M. Goñi, A. Gulik, R. Vargas and V. Luzzati, *FEBS Lett.*, 1995, **368**, 143–147.
22 A. Angelova, M. Ollivon, A. Campitelli and C. Bourgaux, *Langmuir*, 2003, **19**, 6928–6935.

23 J. P. Yang, S. B. Qadri and B. R. Ratna, *J. Phys. Chem.*, 1996, **100**, 17255–17259.
24 P. Nollert, A. Royant, E. Pebay-Peyroula and E. M. Landau, *FEBS Lett.*, 1999, **457**, 205–208.
25 V. Borshchevskiy, E. Moiseeva, A. Kuklin, G. Büldt, M. Hato and V. Gordeliy, *J. Cryst. Growth*, 2010, **312**, 3326–3330.
26 C. J. Drummond and C. Fong, *Curr. Opin. Colloid Interface Sci.*, 2000, **4**, 449–456.
27 S. Engström, T. P. Nordén and H. Nyquist, *Eur. J. Pharm. Sci.*, 1999, **8**, 243–254.
28 J. M. Boggs, *Biochem. Cell Biol.*, 1986, **64**, 50–57.
29 I. D. Pogozheva, H. I. Mosberg and A. L. Lomize, *Protein Sci.*, 2014, **23**, 1165–1196.
30 J. Pedrós, C. M. Gómez, A. Campos and C. Abad, *Spectrochim. Acta, Part A*, 1997, **53**, 2219–2228.
31 *Molecular Drug Properties: Measurement and Prediction*, ed. R. Mannhold, Wiley-VCH, Weinheim, 2008.
32 *Chemical Biology: From Small Molecules to System Biology and Drug Design*, ed. S. L. Schreiber, T. M. Kapoor and G. Wess, Wiley-VCH, Weinheim, 2007.
33 *Comprehensive Medicinal Chemistry II: Computer Assisted Drug Design*, ed. J. S. Mason, Elsevier, Oxford, 2006.
34 Y. Jin, L. Song, Y. Su, L. Zhu, Y. Pang, F. Qiu, G. Tong, D. Yan, B. Zhu and X. Zhu, *Biomacromolecules*, 2011, **12**, 3460–3468.
35 P. D. Dobson and D. B. Kell, *Nat. Rev. Drug Discovery*, 2008, **7**, 205–220.
36 C. A. Lipinski, *J. Pharmacol. Toxicol. Methods*, 2000, **44**, 235–249.
37 N. I. Zahid, O. K. Abou-Zied and R. Hashim, *J. Phys. Chem. C*, 2013, **117**, 26636–26643.
38 C. Xu, J. Fan, W. Riekhof, J. E. Froehlich and C. Benning, *EMBO J.*, 2003, **22**, 2370–2379.
39 U. Kragh-Hansen, *Pharmacol. Rev.*, 1981, **33**, 17–53.
40 T. Peters Jr, *Adv. Protein Chem.*, 1985, **37**, 161–245.
41 A. Sankaranarayanan, G. Raman, C. Busch, T. Schultz, P. I. Zimin, J. Hoyer, R. Köhler and H. Wulff, *Mol. Pharmacol.*, 2009, **75**, 281–295.
42 H. Razavi, S. K. Palaninathan, E. T. Powers, R. L. Wiseman, H. E. Purkey, N. N. Mohamedmohaideen, S. Deechongkit, K. P. Chiang, M. T. Dendle, J. C. Sacchettini and J. W. Kelly, *Angew. Chem., Int. Ed.*, 2003, **115**, 2864–2867.
43 T. Grandi, F. Sparatore, C. Gnerre, P. Crivori, P.-A. Carrupt and B. Testa, *AAPS PharmSci*, 1999, **1**, 1–4.
44 G. J. Woolfe, M. Melzig, S. Schneider and F. Dörr, *Chem. Phys.*, 1983, **77**, 213–221.
45 O. K. Abou-Zied, R. Jimenez, E. H. Z. Thompson, D. P. Millar and F. E. Romesberg, *J. Phys. Chem. A*, 2002, **106**, 3665–3672.
46 H. Wang, H. Zhang, O. K. Abou-Zied, C. Yu, F. E. Romesberg and M. Glasbeek, *Chem. Phys. Lett.*, 2003, **367**, 599–608.
47 T. Arthen-Engeland, T. Bultmann, N. P. Ernsting, M. A. Rodriguez and W. Thiel, *Chem. Phys.*, 1992, **163**, 43–53.
48 P. F. Barbara, L. E. Brus and P. M. Rentzepis, *J. Am. Chem. Soc.*, 1980, **102**, 5631–5635.
49 K. Ding, S. J. Courtney, A. J. Strandjord, S. Flom, D. Friedrich and P. F. Barbara, *J. Phys. Chem.*, 1983, **87**, 1184–1188.
50 M. Itoh and Y. Fujiwara, *J. Am. Chem. Soc.*, 1985, **107**, 1561–1565.
51 O. K. Abou-Zied, *Chem. Phys.*, 2007, **337**, 1–10.
52 N. I. Zahid, C. E. Conn, N. J. Brooks, N. Ahmad, J. M. Seddon and R. Hashim, *Langmuir*, 2013, **29**, 15794–15804.
53 P. Sakya and J. Seddon, *Liq. Cryst.*, 1997, **23**, 409–424.
54 G. E. Schröder-Turk, L. de Campo, M. E. Evans, M. Saba, S. C. Kapfer, T. Varslot, K. Grosse-Brauckmann, S. Ramsden and S. T. Hyde, *Faraday Discuss.*, 2013, **161**, 215–247.
55 G. C. Shearman, O. Ces, R. H. Templer and J. M. Seddon, *J. Phys.: Condens. Matter*, 2006, **18**, S1105.
56 R. Hashim, H. H. A. Hashim, N. Z. M. Rodzi, R. S. D. Hussen and T. Heidelberg, *Thin Solid Films*, 2006, **509**, 27–35.
57 O. K. Abou-Zied, N. I. Zahid, M. F. Khyasudeen, D. S. Giera, J. C. Thimm and R. Hashim, *Sci. Rep.*, 2015, **5**, 8699.
58 F. Nilsson, O. Söderman and I. Johansson, *Langmuir*, 1996, **12**, 902–908.
59 M. G. Bonicelli, G. F. Ceccaroni and C. la Mesa, *Colloid Polym. Sci.*, 1998, **276**, 109–116.
60 N. I. Zahid, O. K. Abou-Zied, R. Hashim and T. Heidelberg, *J. Phys. Chem. C*, 2011, **115**, 19805–19810.
61 N. I. Zahid, O. K. Abou-Zied, R. Hashim and T. Heidelberg, *Langmuir*, 2012, **28**, 4989–4995.
62 O. K. Abou-Zied, *J. Photochem. Photobiol., A*, 2006, **182**, 192–201.
63 D. R. James, A. Siemiarczuk and W. R. Ware, *Rev. Sci. Instrum.*, 1992, **63**, 1710–1716.
64 O. K. Abou-Zied, R. Jimenez and F. E. Romesberg, *J. Am. Chem. Soc.*, 2001, **123**, 4613–4614.
65 F.-Y. Dupradeau, D. A. Case, C. Yu, R. Jimenez and F. E. Romesberg, *J. Am. Chem. Soc.*, 2005, **127**, 15612–15617.
66 O. K. Abou-Zied, *Phys. Chem. Chem. Phys.*, 2012, **14**, 2832–2839.
67 O. K. Abou-Zied, *RSC Adv.*, 2013, **3**, 8747–8755.
68 J. E. Hansen, E. Pines and G. R. Fleming, *J. Phys. Chem.*, 1992, **96**, 6904–6910.
69 P. Chowdhury, S. Panja, A. Chatterjee, P. Bhattacharya and S. Chakravorti, *J. Photochem. Photobiol., A*, 2005, **170**, 131–141.
70 J. Kim, W. Lu, W. Qiu, L. Wang, M. Caffrey and D. Zhong, *J. Phys. Chem. B*, 2006, **110**, 21994–22000.
71 T. Plat and R. J. Linhardt, *J. Surfactants Deterg.*, 2001, **4**, 415–421.
72 R. D. Dennis, G. Lochnit and R. Geyer, in *Glycoanalysis Protocols*, Springer, 1998, pp. 197–212.
73 Z. Huang, W. Teng, L. Liu, L. Wang, Q. Wang and Y. Dong, *Nanotechnology*, 2013, **24**, 265104.